

Morphology and structural phase transitions of Pd monolayers on Ta(110)

M. W. Ruckman, V. Murgai,* and Myron Strongin

Department of Physics, Brookhaven National Laboratory, Upton, New York 11973-5000

(Received 29 May 1986)

The morphology of Pd overlayers on Ta(110) was studied for various Pd coverages before and after heat treatment. As was reported for Pd on Nb(110), a structural phase transition from a commensurate epitaxial overlayer to an incommensurate overlayer was found at approximately one monolayer (ML) coverage (1 ML = 1.89 Å). Valence-band photoemission and Auger-electron energy distribution curves show modifications of the Pd-derived valence-band states attributable to Pd—Ta bonding and reduced Pd nearest-neighbor coordination. Little change is seen in the Pd density of states during the commensurate-incommensurate transition. Thicker Pd layers ($\theta > 1$ ML) evolve toward the structure and photoemission properties characteristics of Pd(111). Thermal treatment of the thick Pd overlayer triggered the interdiffusion of Ta and Pd and produced an extended Pd-Ta surface compound. Further heat treatments caused additional Pd and Ta interdiffusion and left a surface-retained Pd “monolayer” with the same structure as the Ta(110) substrate.

INTRODUCTION

Metal overlayers deposited on transition-metal surfaces exhibit a rich variety of phenomena that have attracted recent interest.^{1–6} We have been particularly interested in the effect on the surface chemical properties of refractory metals modified by the deposition of noble and near-noble transition metals.^{7,8} Although our previous work focused on studies of Pd layers on Nb(110), we have extended our work to Pd on Ta(110) to test the generality of the phenomena observed for Pd/Nb and its effect on the reactivity of Ta and Pd surfaces. These studies not only include a careful characterization of the structure of the Pd overlayer during deposition and subsequent heat treatment, but also include an examination of the ensuing changes in the electronic structure as derived from photoelectron spectroscopy.

Our interest in this particular system is in part a natural extension of previous studies of Pd (Ref. 7) and Cu (Ref. 8) overlayers on Nb(110) and their effect on the bulk uptake of hydrogen,⁵ and is also due to the fact that the sharp 4*f* Ta core levels lie within 30 eV of the Fermi level (E_F).⁹ The attenuation of these core levels can be used as a probe of the overall morphology of the overlayer and can detect very small levels of Ta diffusion across the interface. The sensitivity of these sharp 4*f* levels to modifications of the valence band raises the possibility of using the Ta 4*f* core levels to detect the formation of new Ta, Pd, and Ta—Pd bonding environments. Like Nb, the rate of hydrogen uptake by Ta is significantly increased by the deposition of several layers of Pd on the surface.⁵ Recent work on the transition-metal overlayer systems, Pd on Mo(110) and W(110) (Ref. 4) shows that the addition of a monolayer of Pd sharply reduces the saturation coverage of CO at room temperature. We found this to be true for the Pd/Ta(110) surface.¹⁰ Our investigation of the structure and electronic properties Pd on Ta(110) could provide some basis for understanding this phenomenon.

EXPERIMENTAL

In the current investigation, low-energy electron diffraction (LEED) was used to determine the structure of the Pd overlayer; Auger-electron spectroscopy (AES) was used to measure the Pd coverage or overlayer thickness and to ensure surface cleanliness; and angle-integrated photoelectron spectroscopy (AIPES) was used to determine the local density of states (LDOS) of the valence band and measure the core-level shifts of the Ta 4*f*_{7/2} and 4*f*_{5/2} levels.

The experiments were performed in two different UHV chambers (base pressures in the mid 10^{−10} Torr range)—one with a gas discharge lamp providing He I (21.2 eV) light and the other obtaining light from the vuv ring at the National Synchrotron Light Source (NSLS) at Brookhaven National Laboratory. Photoemission spectra were measured using a double pass cylindrical mirror analyzer with an energy resolution of ≈ 0.25 eV. The samples used were 0.001-in.- or 0.002-in.-thick foils of Ta (Marz grade from Materials Research Corporation) which were recrystallized into visible grains showing the (110) face of Ta as checked by low-energy electron diffraction (LEED). The recrystallization was performed by heating the sample to 1000 K in O₂ at $\sim 10^{-6}$ Torr for one hour, followed by repeated heating near to its melting temperature (≈ 3000 K). After recrystallization, the sample could be cleaned by flash heating the sample close to its melting temperature. Cleanliness was monitored using Auger-electron spectroscopy (AES) and angle-integrated photoemission which was found to be more sensitive to residual traces of contamination (predominantly oxygen and hydrogen). Pd was evaporated onto the sample from a resistively heated tungsten basket. Deposition rates varied from 0.3 to 1.0 monolayer (ML) per minute. Pd coverage was determined from the intensity of the Ta 179- and Pd 328-eV Auger transitions. The dependence of Auger signal strength versus evaporation time was characteristic of

two-dimensional layer-by-layer growth.¹¹ Heat treatments were done by resistively heating the Ta foil. Sample temperatures were determined by using four probe resistance measurements of the Ta and cross checked with an optical pyrometer.

RESULTS AND DISCUSSION

Low-energy electron diffraction was used to determine whether Pd overlayers of increasing coverage were sufficiently ordered to produce a display LEED pattern. For low coverages, $0 < \Theta \leq 0.5$ ML (1 ML = 1.3×10^{15} atoms/cm²), no additional LEED spots, apart from the distorted hexagonal pattern seen for the clean Ta(110) surface, were observed. The LEED spots maintained their sharpness against a slowly increasing background. These results are consistent with the chemisorption of Pd atoms in continuation sites on the underlying Ta(110) substrate. Since the same LEED pattern exists at a coverage of ~ 0.5 ML, we believe the Pd atoms agglomerate form islands and produce coherent scattering arrays.¹² At greater Pd coverages, $\Theta > 0.5$ ML, new LEED spots, shown photographically in Fig. 1, are superimposed upon the Ta(110) pattern. The new spots form linear arrays of spots centered on the Ta(110) LEED spots and aligned along the shorter axis of the distorted hexagonal pattern produced by the bcc (110) surface. These additional LEED spots, which were also observed for Pd/Nb(110),¹² can be generated by multiple scattering between an incom-



FIG. 1. Display LEED image of an incommensurate Pd monolayer on Ta(110) taken using 128-eV energy primary electrons. Satellite spots attributed to multiple scattering between the overlayer and the substrate are clearly visible.

mensurate Pd(111) overlayer and a Ta(110) substrate. The frequency of the satellite spots or "beats" indicates that the Pd overlayer enters equivalent surface sites every seven surface unit cells. Examination of a close-packed Pd monolayer shows that this is consistent with the lattice constants for unstrained close-packed Ta and Pd planes. The beat pattern is faint at low coverages and grows in intensity with increasing Pd coverage. Once the beat pattern had been established, no further changes in beat spacing was observed. This behavior suggests that two-dimensional islands of incommensurate Pd(111) grow from the Pd*(110) islands established at lower coverage. It is plausible that the Pd*(110) islands undergo a structural relaxation in transforming from Pd*(110) to Pd(111) because the Pd*(110) mesh can be generated by subjecting the Pd(111) mesh to a uniaxial stretch of $\approx 15\%$ along the [001] direction. The Pd*(110) is metastable because the alignment of the overlayer with the Ta(110) substrate introduces considerable strain into the Pd overlayer. The Pd*(110) islands are presumably stabilized by island-edge energy contributions which decrease as the ratio of island edge to interior atoms decreases. Thus, when the islands reach a critical size they might spontaneously transform to the close-packed Pd(111) structure by undergoing a first-order structural phase transition of the type described by Schaub and Mukamel.¹³ The transformation of the island may also be prompted by the introduction of additional Pd atoms into the more open Pd*(110) structure during successive Pd depositions. Finally, the Pd*(110) structure may be disrupted by the possible stacking of Pd atoms on top of the Pd*(110) islands.

The intensity of the beam pattern reaches a maximum of ~ 1 -ML coverage. CO chemisorption studies undertaken by Ruckman *et al.*¹⁰ show that features characteristic of dissociative chemisorption on refractory metal surfaces are absent for ~ 1 ML Pd/Ta(110). Further addition of Pd ($\Theta \geq 1.5$ ML) reduced the intensity of the LEED pattern seen at lower coverages. Diffuse or fuzzy LEED spots arrayed in simple hexagonal network replaced the pattern described earlier. These LEED spots are the same as those seen for single crystal Pd(111). The diffuse quality of the spot pattern suggests that the surface is atomically rough. Thermal treatments failed to produce a smooth recrystallized Pd(111) surface and instead provoked the interdiffusion of Pd and Ta. Our LEED data is consistent with the formation of a polycrystalline Pd layer with preferential Pd(111) orientation along the surface normal and only limited rotational disorder. The morphology we observe for Pd layers deposited on Ta(110) is characteristic of near-noble metals on bcc (110) refractory metal surfaces and has been reported for Pd layers on Nb,¹² Mo and W(110).⁴

Monolayer films of Pd in the Pd(110) structure on Ta(110) can also be created by heating a 3–4 ML thick Pd overlayer to drive the excess Pd into the bulk. Auger spectra were measured after each heating and the resulting Ta and Pd intensities are shown in Fig. 2(a). The horizontal axis shows the annealing temperature. These temperatures were derived assuming that the amount of Pd present is insufficient to change the bulk Ta resistivity. A

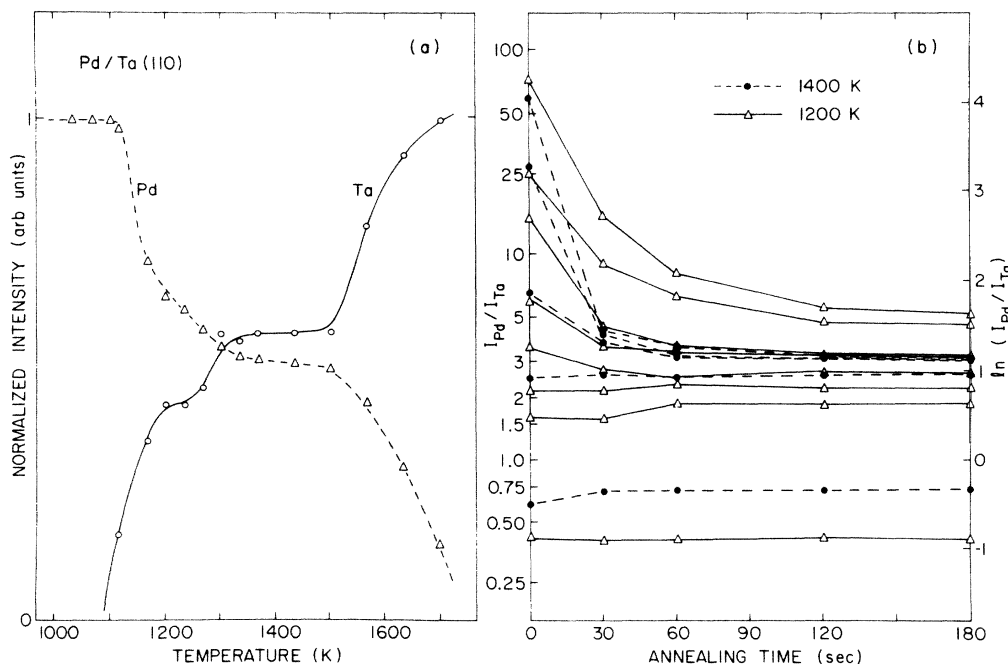


FIG. 2. (a) Peak-to-peak heights of the Pd MNN and Ta NVV Auger lines for a 6 ML thick Pd overlayer during a series of isothermal heat treatments. (b) Ratio (I_{Pd}/I_{Ta}) of the peak-to-peak heights for the Pd and Ta Auger lines for various starting thicknesses of Pd heated to 1200 and 1400 K, respectively.

well-defined and reproducible plateau was observed for both the Ta and Pd. The Pd/Ta surface produced by the heat treatment had the approximate amount of Pd expected for a Pd monolayer (verified by Auger spectroscopy) and was found to be inert to the uptake of CO. The LEED pattern corresponding to the higher temperature plateau, is identical to the Ta(110) pattern and on the basis of these similarities, we tentatively identify the resulting Pd overlayer as a commensurate Pd*(110) layer. The LEED pattern observed for the lower temperature plateau was fuzzy and streaked. Such a pattern could not be reproduced by deposition alone.

Incremental amounts of Pd were added to the Pd*(110) to determine whether the resulting Pd/Ta surface was a surface segregated monolayer as reported by Sagurton *et al.*¹² for Pd/Nb(110), or a Pd/Ta surface compound with a surface structure similar to Pd*(110). Beats as shown in Fig. 1 were induced by the addition of as little as 10–20% more Pd. The rapid onset of the “incommensurate” LEED pattern indicates that a structural phase transition has taken place. If the second layer of Pd was going down in a Pd(111) structure while the first layer retained the rigid Pd*(110) structure, the intensity of the beat pattern would increase in proportion to the increase in Pd coverage in the second layer, which was not observed. Since a Pd(111) layer contains 18% more Pd atoms than a Pd*(110) layer, we conclude that the addition of 20% more Pd atoms was sufficient to permit the entire Pd*(110) monolayer to undergo a structural phase transition to the Pd(111) structure. Since the structural transformation of the thermally stabilized Pd(110)* layer proceeds in the same manner observed for Pd islands or

Ta(110), we believe that the immediate surface layer probably consists only of Pd atoms. An additional mechanism must serve to stabilize the Pd*(110) structure beyond the Pd coverages observed for direct deposition of Pd on Ta(110). The spacing of the beat pattern remains constant which suggests that the incommensurate portion of the Pd overlayer maintains the same structure with increasing Pd coverage. Indicating this is a first-order transition between two distinct phases.

A question that was not fully addressed in the earlier work on Pd/Nb(110) was the mechanism by which the Pd*(110) layer could be produced by heating. Several mechanisms could give rise to Pd*(110). First a monolayer of Pd could be retained on the surface after the bulk of the Pd had diffused into the bulk. Examination of a Darken-Gurry¹⁴ plot for Ta shows that Pd has very limited solubility in Ta, but Ta can readily go into solution in Pd. Another possibility is that an ordered Ta-Pd surface compound could form which, by coincidence, has a surface structure equivalent to Pd*(110). This would imply that the compound consists of alternating layers of Pd and Ta atoms. A final possibility is that Pd could thermally desorb from the surface removing all but one chemisorbed monolayer.

We can examine the thermal stability of Pd layers of varying thickness on Ta(110) to address this question. Figure 2(b) shows the relative amounts of Pd and Ta retained in the surface region probed by Ta NVV (179 eV) and Pd MNN (328 eV) Auger electrons after isothermal annealing at 1200 and 1400 K for varying durations ranging from 30 to 180 s. Annealing for longer than 180 s produced no significant change in the Auger signal

strengths. Hence, we believe that the samples were driven into thermal equilibrium by ~ 180 s. Our data shows that submonolayer coverages of Pd ($I_{\text{Pd}}/I_{\text{Ta}} < 2.8$) are unaffected by heating indicating that very little interdiffusion of Pd and Ta can occur at either 1200 or 1400 K. Significant changes in the relative amounts of Pd and Ta [Fig. 2(a)] were not found to occur until the temperature was increased beyond 1500 K, a temperature high enough for the partial pressure of Pd to reach 10^{-8} Torr. At this temperature Pd could be thermally desorbed from the surface.

Multilayer Pd coverages [Fig. 2(b)] showed reduced amounts of Pd as the annealing time was increased. This is indicative of overlayer/substrate intermixing resulting from either interdiffusion or reactive compound formation. At 1200 K, the heating is unable to drive all combinations of Pd/Ta to the same apparent stoichiometry.

This may be due to real differences in stoichiometry implying that we could form a series of increasingly Pd-rich overlayers by increasing the thickness of Pd. Alternatively, the Pd/Ta overlayer could have fixed stoichiometry but vary in thickness. The variation in apparent amounts of Pd and Ta would cease when the Pd/Ta was sufficiently thick and would stabilize at a concentration characteristic of the Pd/Ta phase actually formed. Increasing the annealing temperature further narrows the range of Pd/Ta overlayers produced. At 1400 K, identified in Fig. 2(a) as the high-temperature plateau, the resulting Pd and Ta AES ratio is virtually independent of the initial Pd thickness and is ~ 3.2 . This value is larger than the value predicted for a Pd*(110) monolayer (~ 2.8). Because the addition of Pd to the Pd*(110) surface, produced by heating, triggers the commensurate-incommensurate transition we conclude that the first layer of atoms is mostly com-

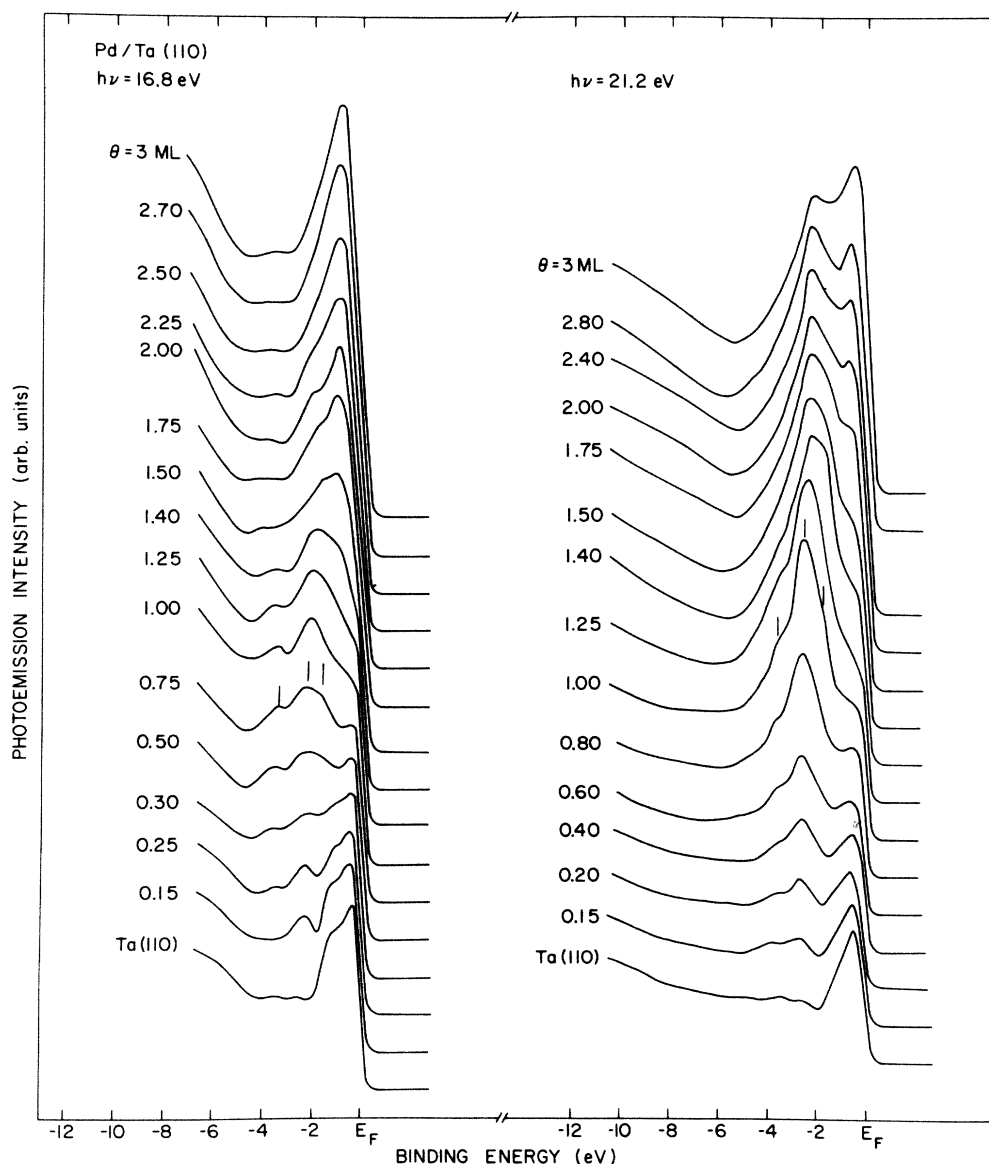


FIG. 3. Photoemission energy distribution curves for various coverages of Pd on Ta(110) at 16.8- and 21.2-eV photon energies.

posed of Pd atoms.

To summarize our results for the thermal treatment of Pd film on Ta(110), we find monolayer and submonolayer coverages do not diffuse into Ta(110) upon heating. They do thermally desorb from the surface if heated beyond 1500 K. Thicker Pd films are modified by processes that introduces Ta into the Pd film when the temperature exceeds 1100 K. Thermal stabilization of the Pd/Ta film probably produces a Ta-rich layer covered by a monolayer of Pd. This Pd monolayer has a structure previously labeled as Pd*(110).

Additional insight into the nature of the Pd/Ta(110) can be derived from photoelectron and Auger spectroscopy. In Fig. 3 we show photoemission energy distribu-

tion curves (EDC) for various coverages of Pd/Ta(110) at the 16.8 eV (NeI) and 21.2 eV (HeI) emission lines. Our results for Pd/Ta(110) are similar to photoemission data and band-structure calculations for Pd/Nb(110) by El-Batanouny *et al.*^{7,15} and valence-band density-of-states calculations by Kumar and Bennemann.¹⁶ Further insights can be derived from studies of Pd silicides and the Pd/Si interfaces which show analogous modification of the Pd valence-band states.

From the $h\nu=16.8$ and 21.2 eV EDC's in Fig. 3, three Pd derived d states located at approximately -1.5 to -1.8 , -2.1 to -2.8 , and -3.5 to -4 eV below the Fermi level characterize the modification of the clean Ta EDC's at lower coverages ($\Theta < 1$ ML). Emission from the

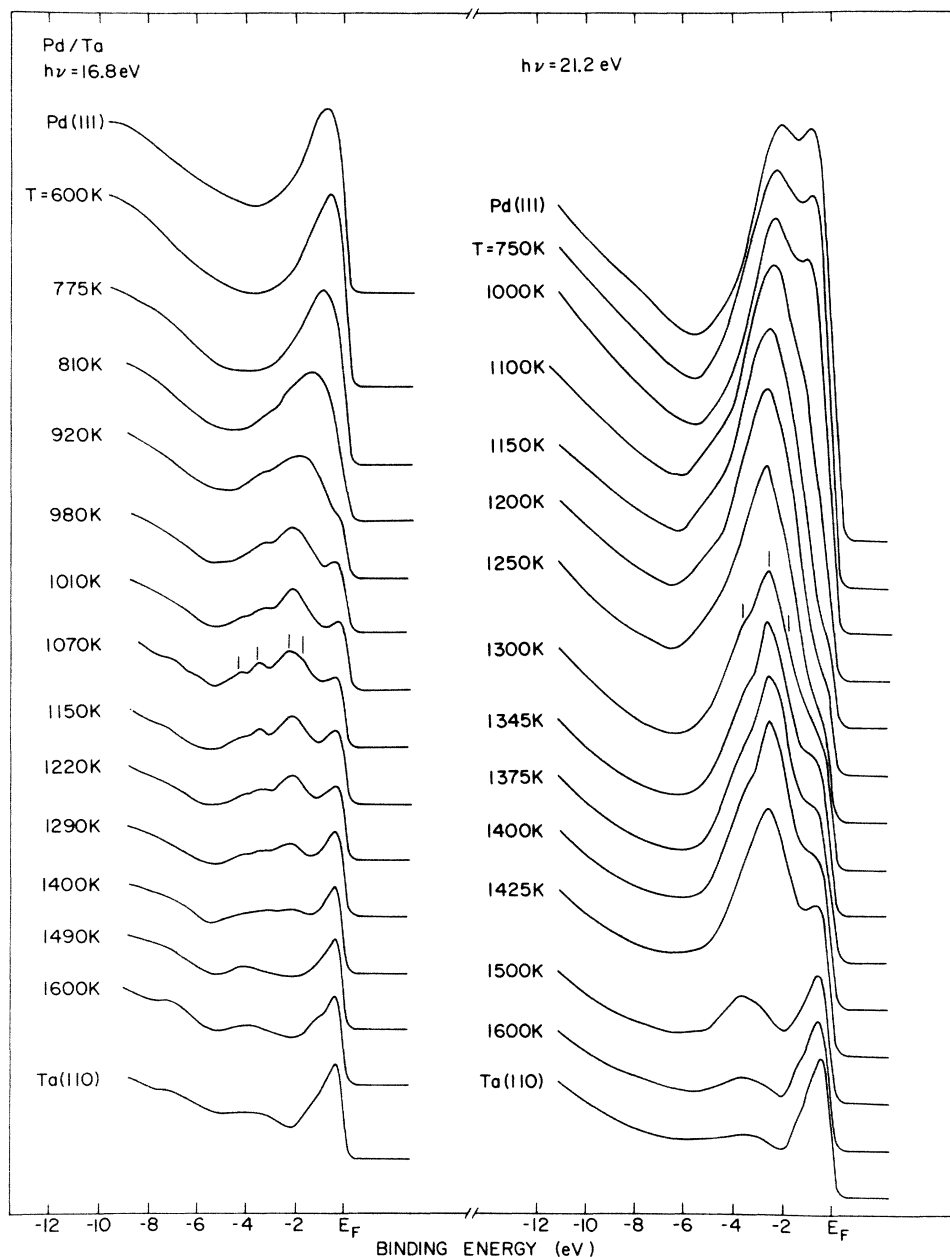


FIG. 4. Photoemission energy distribution curves for a thick (~ 6 ML) Pd overlayer subjected to isothermal heat treatments exceeding 3-min duration taken at 16.8 and 21.2 eV.

−2.1 to −2.8-eV binding-energy state is stronger than the emission from the other two states in both the 16.8- and 21.2-eV spectra. Emission from the Pd-induced states grows relative to the Ta-derived states near E_F for Pd coverages between 0.2 and 1.25 ML.

To interpret our photoemission spectra for Pd/Ta(110) we draw a direct analogy with the calculations and energy state assignments for Pd/Nb(110). Similar studies of Pd on Nb(110) concluded that the state which saturated at lowest coverage could be attributed to photoemission from Nb—Pd bonding orbitals and would therefore contain significant Nb character. The states that continued to grow in intensity were attributed to Pd—Pd bonding. By analogy we conclude that the states near −2.4 and −1.8 eV can be attributed to Pd—Pd bonds, whereas the state near −3.5 eV can be attributed to Ta—Pd bonds. The states nearer E_F are attributed to photoemission from the Ta substrate.

Another interpretation of the nature of the Pd/Ta valence-band states can be gained from an examination of the electron structure of Pd silicides measured for various Pd silicides and Pd/Si interfaces by a number of workers.¹⁷ The Pd/Si valence band shows structural similarity to the Ni silicide density of states reported by Franciosi *et al.*¹⁸ In this case the Ni metal states are shifted further below the Fermi level because the metal d - d overlap is reduced as a consequence of the reduction in Ni metal coordination. Hence the hybridization energy terms that serve to broaden the d band are reduced and the increased localization of the d states in part caused by a reduction screening by the s and p charge increases their binding energy. These states are nonbonding in the sense that they are localized at Ni atom sites. Bonding between metal and Si is partially covalent and occurs between metal s and p states and the Si p states. The s and p charge are localized in bonds between the metal and Si. By analogy with calculations for silicides, we can conclude that the intense Pd states observed for a monolayer are probably nonbonding in character and that the hybrid Pd—Ta bonding states are less intense.

When the Pd coverage exceeds a monolayer, modifications in the valence band suggest that Pd metal begins to agglomerate atop the Nb(110). An additional state detected in the EDC's taken at 16.8 and 21.2 eV appears at increased Pd coverage, i.e., $\Theta > 1.6$ at approximately −0.8 eV below E_F . Studies of Pd films on Nb(110) by Weng and El-Batanouny⁷ suggested that an analogous state could be a surface state or resonance. We have found that this state is sensitive to both sample preparation, contamination and Xe adsorption at cryogenic temperatures,¹⁹ we suggest but cannot conclude that this state is a surface state or resonance. At the thickest Pd coverages the photoemission EDC's assume the shape reported for Pd metal²⁰ (Fig. 3).

Energy distribution curves for annealed Pd/Ta overlayers as a function of temperature at 16.8- and 21.2-eV photon energy are shown in Fig. 4. Auger spectra for a 3–4 ML thick Pd film, an "as-deposited" Pd monolayer, and an annealed Pd "monolayer" are shown in Fig. 5. Rapid evolution of the Pd/Ta valence band is observed as the temperature is increased from 750 to 1000 K. The Pd

density of states shifts away from E_F suggesting that the Pd metal bonding states are being disrupted. Auger spectra [Fig. 2(a)] show that Ta is being introduced into the Pd overlayer. Therefore, our spectra show that a Pd/Ta surface alloy or compound is being formed. The overall appearance of our valence-band spectra for annealed Pd/Ta is consistent with spectra presented by Fuggle *et al.*²¹ for Pd/Ta alloys studied using x-ray photoemission spectroscopy. Since our spectra can be fitted by a superposition of "reacted" Pd and unreacted Pd metal, we believe that an intermetallic surface phase forms. This conclusion is reinforced by an examination of the Pd MNN Auger lines shown in Fig. 5 and the Ta 4*f* core levels shown in Fig. 6. The Pd/Ta surface component in Fig. 6 can be fitted by a single Ta 4*f* core-level component shifted 0.7 eV higher in binding energy. A chemical shifted Auger component is observed on the lower kinetic energy edge of MNN (328 eV) Pd line. Comparison of the Ta 4*f* core and Pd line for the vapor deposited Pd/Ta interface and the overlayer produced by heating shows that the shifted components observed in both cases are virtually identical, and indicate that the Pd—Ta bonding is similar in both cases.

The similarity in electronic structure is seen in a comparison of the valence bands (Fig. 4) observed for the

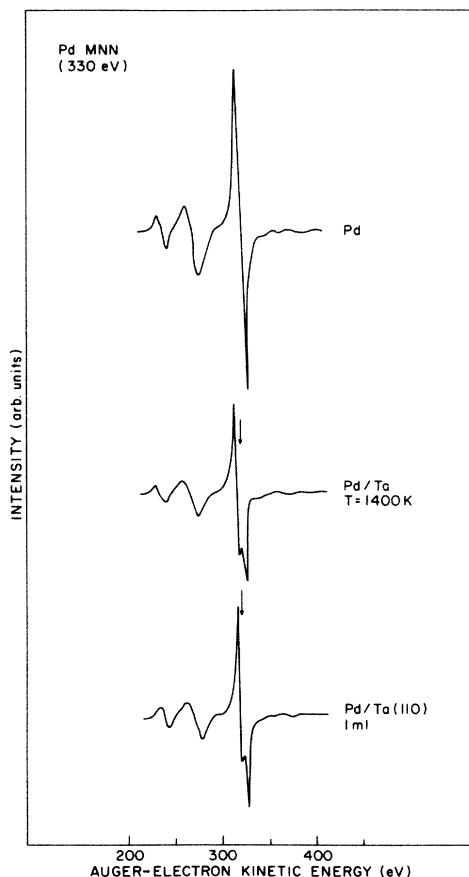


FIG. 5. Derivative Auger spectra showing the 330-eV Pd MNN Auger transition for a Pd metal film, for a thermally stabilized Pd*(110) surface (~ 1400 K) and for an incommensurate Pd(111) monolayer on Ta(110).

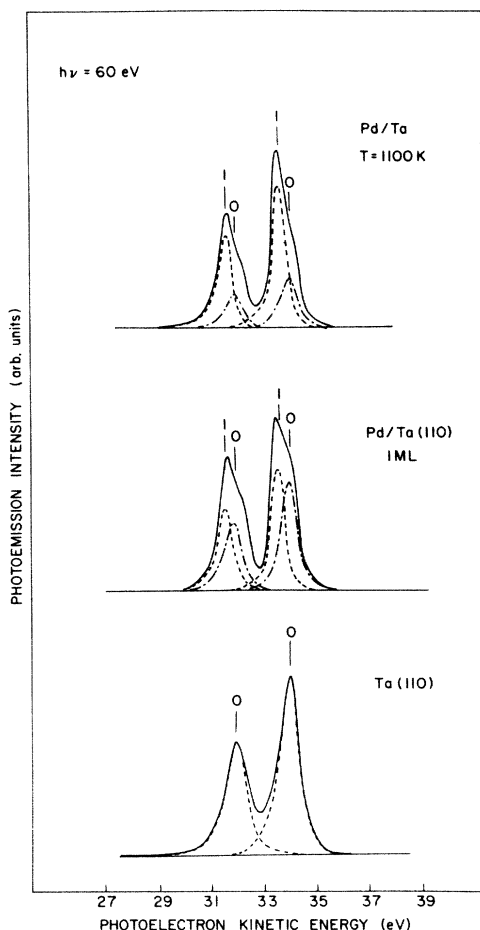


FIG. 6. Characteristic Ta $4f_{7/2}$ and $4f_{5/2}$ core-level spectra taken for a clean Ta surface, one covered with an incommensurate Pd(111) monolayer on Ta(110) and another taken for a thermally stabilized Pd*(110) surface (~ 1400 K).

Pd/Ta interface and the fully stabilized (high-temperature plateau) Pd/Ta surface layer. The same Pd-induced states at near -3.5 , -2.4 , and -1.8 eV are observed. Evidence for a fourth state near -4.5 eV is seen in the 16.8-eV spectra for the annealed Pd/Ta overlayer. The relative intensity of the -3.5 -eV state previously identified with Pd-Ta bonding is greater for the Pd/Ta surface compound. A more thorough examination of the Auger spectra (Fig. 5) shows that relative intensity of the chemically shifted component is greater for the Pd/Ta surface compound than for the Pd/Ta(110) interface. The unshifted Pd Auger component systematically increased in intensity with incremented Pd depositions once the Pd coverage exceeded ~ 0.6 ML. Although it is difficult to draw conclusions about the Auger line shape from derivative Auger spectra we believe that the growth of the unshifted Pd component indicates that Pd-Pd bonds are being formed. Comparison of the photoemission from approximate monolayer coverages of Pd on Ta for the incommensurate Pd(111) layer produced by evaporation and the Pd*(110)

produced by deposition plus heat treatment show that the Pd electronic structure has the same general features for both Pd structures but also shows detailed differences probably attributable to the Pd packing density in the monolayer.

The critical difference in interface morphology between Pd/Ta(110) and the thermally induced Pd monolayer on Ta is best illustrated by decomposition of the Ta $4f$ core levels shown in Fig. 6. The Ta $4f$ levels are not involved in the bonding to the Pd atoms, or Ta atoms for that matter. In Fig. 6 the Ta $4f$ levels for clean Ta are shown. When Pd is added the peaks can be decomposed into two peaks, one from bulk Ta and one feature from the interaction of Ta and Pd. From an analysis of the bulk and shifted peaks one can get some idea of relative Pd distributions. For example, the relative intensity of the undisturbed Ta $4f_{7/2}$ and $4f_{5/2}$ component attributable to the Ta substrate is much reduced for the thermally annealed Pd/Ta as compared to a Pd/Ta(110) monolayer. Since the overall area of the Ta $4f_{7/2}$ peaks are comparable, this demonstrates that some Pd must be dispersed under the surface-retained Pd(110) layer. The modification of the substrate from Ta(110) to a tantalum-rich alloy or solid solution with Pd must stabilize the Pd*(110) surface, since our results show that the commensurate-to-incommensurate transition for vapor-deposited Pd island occurs at submonolayer coverage.

SUMMARY

To summarize our results we found that Pd overlayers initially go down in a commensurate structure on Ta(110). The electronic structure of the Pd*(110) layer is heavily modified suggesting that strong chemisorption bonds form. The overlayer relaxes into the incommensurate close-packed Pd(111) structure at submonolayer coverage. Surface completion coverage occurs at approximately a monolayer. Polycrystalline Pd is deposited on top of the first deposited Pd monolayer. Heating a thick Pd overlayer triggered interdiffusion and reaction to form a Pd/Ta surface compound. Further heating caused more interdiffusion of Pd and Ta. All but one layer of Pd was removed from the surface and this layer had the Pd*(110) structure observed for lower Pd coverages deposited by evaporation.

ACKNOWLEDGMENTS

We would like to acknowledge many useful discussions with J. W. Davenport and R. E. Watson. We are also indebted to F. Loeb, P. Heilig, and G. Hrabak for technical support. A portion of this work was performed at the vuv ring of the National Synchrotron Light Source (NSLS) and we gratefully acknowledge the support of their staff. This work was supported by the U.S. Department of Energy under Contract No. DE-AC02-76CH00016.

- *Permanent address: Department of Physics, Boston University, Boston, MA 02215.
- ¹P. E. Joynson, in *Handbook of Thin Film Technology*, edited by L. I. Naissel and R. Glanz (McGraw-Hill, New York, 1970).
- ²H. P. Bonzel, *Surf. Sci.* **68**, 236 (1977).
- ³J. P. Biberian and G. A. Somorjai, *J. Vac. Sci. Technol.* **16**, 2073 (1979); G. A. Somorjai and M. A. Van Hove, *Struct. Bonding (Berlin)* **38**, 1 (1979).
- ⁴H. Poppa and F. Soria, *Phys. Rev. B* **27**, 8 (1983); **27**, 5166 (1983); D. Prigge, W. Schlerk, and E. Bauer, *Surf. Sci. Lett.* **123**, L698 (1982).
- ⁵M. Pick, J. W. Davenport, M. Strongin, and G. J. Dienes, *Phys. Rev. Lett.* **43**, 286 (1979); M. Strongin, M. El-Batanouny, and M. Dick, *Phys. Rev. B* **22**, 3126 (1980); M. Sagurton, M. Strongin, F. Jona, and J. Colbert, *ibid.* **28**, 4075 (1985).
- ⁶D. L. Weissman-Wenocur, P. M. Stefan, B. B. Pate, M.-L. Shek, I. Lindau, and W. E. Spicer, *Phys. Rev. B* **27**, 3308 (1983).
- ⁷M. El-Batanouny, P. R. Hamann, S. R. Chubb, and J. W. Davenport, *Phys. Rev. B* **27**, 2575 (1983); S.-L. Weng and M. El-Batanouny, *Phys. Rev. Lett.* **44**, 612 (1980).
- ⁸M. El-Batanouny and M. Strongin, *Phys. Rev. B* **31**, 8, 4798 (1985).
- ⁹*Photoemission in Solids II*, edited by L. Ley and M. Cardona (Spring-Verlag, New York, 1979).
- ¹⁰M. Ruckman and M. Strongin, *Phys. Rev. B* **29**, 7105 (1984); M. Ruckman, P. D. Johnson, and M. Strongin, *ibid.* **31**, 3405 (1985).
- ¹¹G. E. Rhead, *J. Vac. Sci. Technol.* **13**, 603 (1976); M. G. Barthes and G. E. Rhead, *J. Phys. D* **13**, 747 (1980).
- ¹²M. Sagurton, M. Strongin, F. Jona, and J. Colbert, *Phys. Rev. B* **28**, 4075 (1985).
- ¹³B. Schaub and D. Mukammel, *J. Phys. C* **16**, L225 (1983).
- ¹⁴L. Darken and R. Gurry, *Physical Chemistry of Metals* (McGraw-Hill, New York, 1953).
- ¹⁵M. El-Batanouny, M. Strongin, and G. P. Williams, *Phys. Rev. B* **27**, 4580 (1983).
- ¹⁶V. Kumar and K. H. Bennemann, *Phys. Rev. B* **26**, 7004 (1983); **28**, 3138 (1983).
- ¹⁷J. L. Freeouf, G. W. Rubloff, P. S. Ho, and T. S. Kuan, *Phys. Rev. Lett.* **43**, 1836 (1979).
- ¹⁸A. Franciosi, J. H. Weaver, D. G. O'Neill, V. Chabal, J. E. Rowe, J. M. Poate, O. Bisi, and C. Calandra, *J. Vac. Sci. Technol.* **21**, 624 (1982).
- ¹⁹S. Raaen, M. Ruckman, and M. Strongin *Phys. Rev. B* **31**, 623 (1985).
- ²⁰D. R. Lloyd, C. M. Quinn, and N. V. Richardson, *Surf. Sci.* **63**, 174 (1977); N. Dahlbäck, P. O. Nilsson, and M. Pessa, *Phys. Rev. B* **19**, 5961 (1979).
- ²¹J. C. Fuggle, F. U. Hillebrecht, R. Zeller, Z. Zolnierck, P. A. Bennett, and Ch. Freiberg, *Phys. Rev. B* **27**, 2145 (1983); F. U. Hillebrecht, J. C. Fuggle, P. A. Bennett, and Z. Zolnierck, *ibid.* **27**, 2179 (1983).

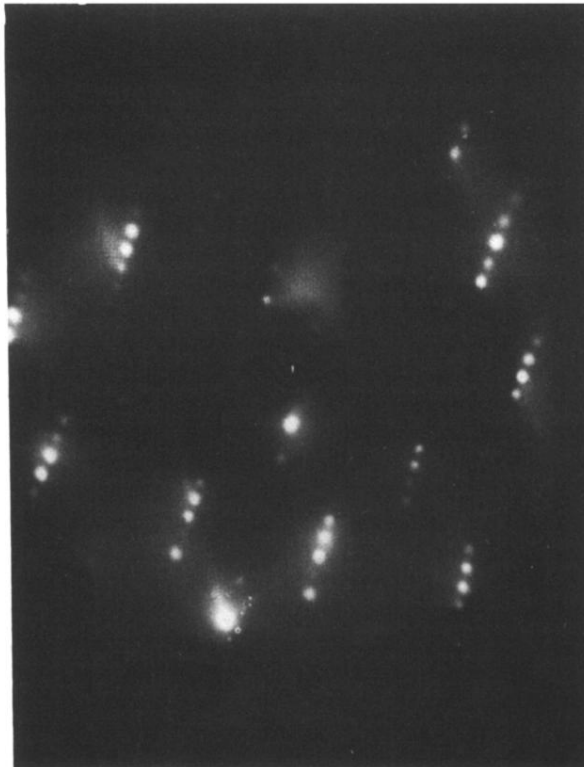


FIG. 1. Display LEED image of an incommensurate Pd monolayer on Ta(110) taken using 128-eV energy primary electrons. Satellite spots attributed to multiple scattering between the overlayer and the substrate are clearly visible.